

Determination of iron burning velocity using the 20-L sphere

Clement Chanut*, Frederic Heymes

Laboratoire des Sciences des Risques, IMT Mines Ales, Ales, France

*clement.chanut@mines-ales.fr

Numerical simulations are used to predict the consequences of dust explosions. One key parameter for modelling the flame propagation is the burning velocity. This velocity represents the consumption rates of the reactant by the flame front. The burning velocity depends on the characteristics of the mixture and on the characteristics of the flow (especially the turbulence characteristics). Experiments are needed to determine the relationship between the burning velocity and the characteristics of the turbulence.

In this paper, experiments in the standardized 20-Liter explosion sphere are performed to study the burning velocity of iron dust. Burning velocity is deduced from the evolution of the pressure inside the closed vessel. Different tests with different ignition delays (i.e. different times between the end of the dust dispersion and the ignition of the mixture) are performed. Indeed, the turbulence intensity at the moment of ignition varies according to this ignition delay. Thus, the influence of turbulence intensity on the burning velocity can be analysed and a relationship between these two quantities can be proposed.

1. Introduction

Dust explosion is a hazard of major concern in industries dealing with powders. Modelling the consequences of such an explosion is still tricky, especially in the case of metallic dusts. Many studies focus on the experimental determination of sensitivity and severity parameters by performing tests in standardized setups, such as the Hartmann tube, or the 20L explosion sphere (Santandrea et al., 2019). These parameters are useful for analysing this risk, they are not sufficient to understand the phenomena of flame propagation and to model accurately the consequences of an accident in real conditions.

To predict the consequences of a real accident, numerical simulations are needed. These simulations are based on the modelling of the flame propagation process. Several models exist to predict the consequences of accidental gas explosions and seem also adapted to organic dust explosions. Nevertheless, these models are not accurate for predicting the consequences in the case of metallic dust explosions (Kahlili, 2012). One key parameter for modelling explosions, and the flame propagation process is the burning velocity. This quantity represents the consumption rate of the reactants by the flame front. Experiments are thus mandatory to estimate this burning velocity during metallic dust explosions.

The burning velocity (S_u) depends on the characteristic of the mixture, via the laminar burning velocity (S_u^0), and on the characteristics of the flow, especially the turbulence level represented for example by the RMS fluctuations velocity (V_{RMS}). Many relations between these three quantities have been proposed in the literature. For example, the following general relation is proposed by Dahoe (2000):

$$\frac{S_u}{S_u^0} = 1 + C \cdot \left(1 + \frac{V_{RMS}}{S_u^0}\right)^n \quad (1)$$

In this paper, confined explosions of iron dusts are studied inside the 20-L sphere. From these tests, severity parameters are first deduced. The severity parameters are: the maximum overpressure (P_{max}) and the maximum rate of pressure rise ($(dP/dt)_{max}$). Burning velocity is also deduced from the evolution of the pressure inside the vessel, applying the method presented by Faghieh and Chen (2016). Different tests are realized at different ignition delay times. The ignition delay time represents the time between the end of the dust dispersion and the ignition of the cloud. The turbulent intensity at the moment of ignition depends on this

ignition delay: the shorter the ignition delay time, the higher the turbulent intensity. The influence of turbulent intensity on iron burning velocity is thus investigated.

2. Materials and Methods

2.1 Presentation of the experiments

Iron dust of 5.1 μm median diameter is studied ($d_{10} = 2.7 \mu\text{m}$; $d_{50} = 5.1 \mu\text{m}$; $d_{90} = 9.8 \mu\text{m}$). Particle size distribution, obtained using a laser particle sizer in air flow (LS13320 Multi-Wave, Beckman Coulter), is exposed on Figure 1 with also an image of the particle shape, recorded with a scanning electron microscope (Quanta 200 Feg, FEI Company).

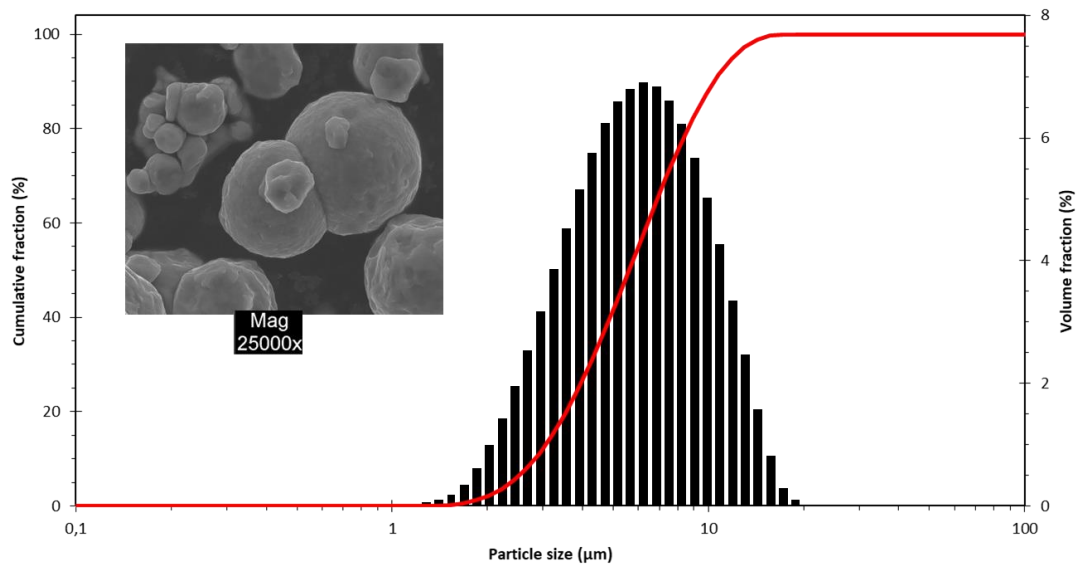


Figure 1: Particle size distribution and image of the particle shape of the iron dust

Iron explosion tests are performed within the standardized 20L explosion sphere (Figure 2); detail of this standardized setup can be found in Kahlili (2012). Iron dust is dispersed by the discharge of a 0.6 L vessel pressurized up to 20 bar. A mushroom nozzle is implemented to improve the dust dispersion inside the sphere.

After an adjustable delay, the iron cloud is ignited by an electrical spark between two electrodes located at the center of the sphere. The energy of the spark is 5 J. The distance between the electrodes is 6 mm.



Figure 2: Photo of the explosion sphere

The evolution of the pressure inside the vessel is recorded by two pressure sensors. An example of pressure evolution recorded during a test is exposed on Figure 3. Before the discharge of compressed air to disperse the iron dust, the sphere is under vacuum. By this way, the sphere is at atmospheric pressure at the moment

of ignition. After ignition, the pressure inside the vessel increase up to the maximum pressure (P_{max}). At the inflection point, the pressure rise reaches its maximum value $((dP/dt)_{max})$. After the pressure has reached its maximum value, the pressure decreases inside the vessel due to heat losses.

The burning velocity can be deduced from this evolution of pressure inside the vessel, using the “Constant Volume Method” described by Faghii and Chen (2016). The burning velocity (S_u) is determined by the following equation:

$$S_u = \frac{R}{3} (1 - (1 - x) \cdot \left(\frac{P_0}{P}\right)^{1/\gamma})^{-2/3} \cdot \left(\frac{P_0}{P}\right)^{1/\gamma} \cdot \frac{dx}{dt} \quad (2)$$

where R is the radius of the sphere, P_0 is the atmospheric pressure, P is the pressure recorded inside the explosion sphere and x is the burned mass fraction. This burned mass fraction is defined as the ration between the mass of burned gas and the mass of unburned gas. Different correlations exist to determine this burned mass fraction. For this study the following equation is used:

$$x = \frac{P - P_0}{P_{max} - P_0} \quad (3)$$

where P_{max} is the maximum pressure recorded.

The value of S_u depends on the pressure inside the vessel. The value corresponding to the inflection point of the curve of pressure evolution inside the vessel is defined as the burning velocity.

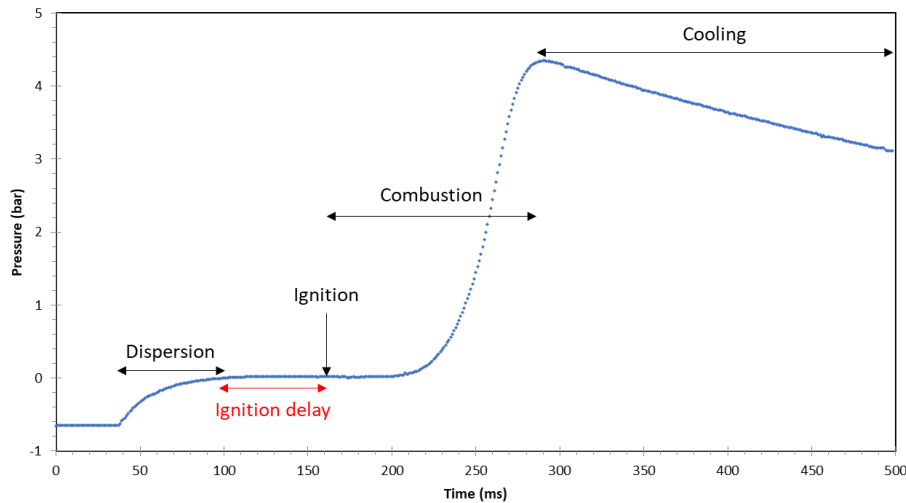


Figure 3: Evolution of pressure over time in the 20L sphere

3. Results

Two iron concentrations corresponding to fuel-rich suspensions are studied: 900 kg.m^{-3} and 1100 kg.m^{-3} . Four ignition delays are studied: 40 ms, 60 ms, 80 ms and 100 ms after the end of the dust dispersion process. For each configuration, 2 tests are realized; 16 tests are thus analyzed in this part.

3.1 Maximum overpressure and maximum rate of pressure rise

Two iron concentrations are studied: 900 g.m^{-3} and 1100 g.m^{-3} . The influence of the ignition delay on the maximum overpressure (P_{max}) and on the maximum rate of pressure rise $((dP/dt)_{max})$ for each concentration is exposed on Figure 4.

A decrease of the maximum rate of pressure rise with the rising ignition delay is observed. This decrease is due to a decrease of the burning velocity with the decreasing turbulent intensity. The maximum overpressure slightly decreases with the rising ignition delay. This decrease is due to an increase of the thermal losses at the walls of the prototype, as the explosion duration is longer (due to a decreasing burning velocity).

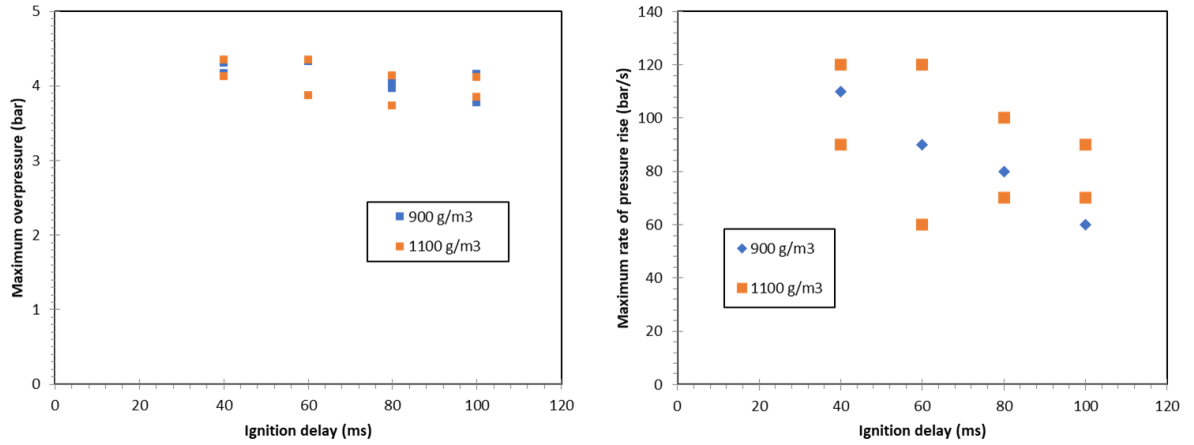


Figure 4: Influence of ignition delay on maximum overpressure (left) and maximum rate of pressure rise (right)

Considering the studied concentrations, no significant influence of concentration on the maximum overpressure and the maximum rate of pressure rise is observed, in comparison with the repeatability of the results. This is consistent with theoretical and experimental results establishing no variations of flame speed in dust clouds with variations of concentration in the case of fuel-rich suspensions (Tang et al., 2009).

For the determination of the relation between the burning velocity and the turbulence intensity, all the experiments are thus analysed without considering the changes in concentrations; only the influence of the ignition delay is studied.

3.2 Determination of burning velocity

Evolution of the burning velocity with the ignition delay is exposed on Figure 5 (left). The errors bars on Figure 5 (left) represents the standard deviation between the four tests. A decrease of the burning velocity with the rising of the ignition delay is observed; from 1.1 m.s⁻¹ for the ignition delay of 40 ms to 0.7 m.s⁻¹ for the ignition delay of 100 ms.

The variations in the ignition delays correspond to variations of the initial turbulent intensity at the moment of ignition. Dahoe et al. (2001) widely studied the dust dispersion process inside the standardized 20L explosion sphere. These authors formulate the following general equation to estimate the turbulent intensity from the ignition delay:

$$\frac{u'_{RMS}}{u'_{RMS}^0} = \left(\frac{t}{t_0}\right)^n \quad (4)$$

where u'_{RMS} is the turbulent intensity after the considered ignition delay, u'_{RMS}^0 is the turbulent intensity immediately after the end for the dispersion process (closure of the valve), t is the considered ignition delay time. t_0 and n are two parameters depending on the nozzle implemented on the sphere. For the mushroom nozzle used in these experiments, these authors proposed a value of n of -1.52 and a value of t_0 of 0.06 s. Evolution of the burning velocity with this estimated turbulent intensity is exposed on Figure 5 (right). An increase of the burning velocity with the turbulent intensity is observed; from 0.7 m.s⁻¹ for a turbulent intensity of 1.3 m.s⁻¹ up to 1.1 m.s⁻¹ for a turbulent intensity of 5.2 m.s⁻¹.

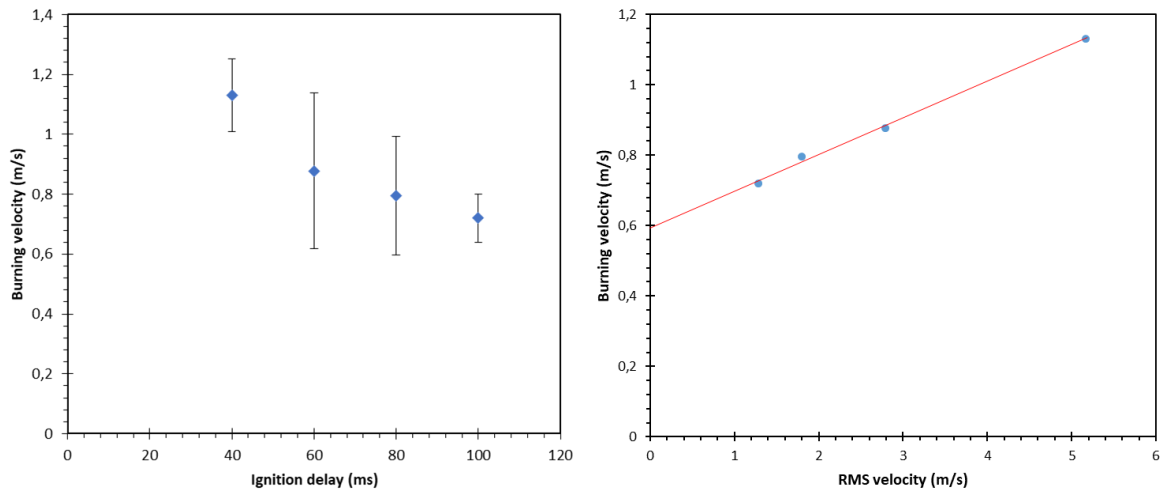


Figure 5: Influence of turbulence on the burning velocity

A linear regression is used to fit the data. An estimated laminar burning velocity (S_u^0) corresponding to a null turbulent intensity is thus obtained; its value is 60 cm.s^{-1} .

Tang et al. (2009) also studied combustion of iron dust with concentrations from 900 to 1200 kg.m^{-3} . They realized experiments in microgravity inside a parabolic flight. They studied the iron flame propagation in tubes. Iron flame velocity of 56 cm.s^{-1} and 20 cm.s^{-1} were obtained with diameter of respectively $3.3 \mu\text{m}$ and $7.0 \mu\text{m}$. Even if the results presented in this paper are based on a different experimental method, the results are consistent.

Furthermore, Broumand and Bidabadi (2013) studied iron dust combustion with a numerical approach. For particle diameter of $5 \mu\text{m}$, they obtained flame velocity of 42 cm.s^{-1} , 49 cm.s^{-1} and 55 cm.s^{-1} for iron concentrations of respectively 500 g.m^{-3} , 600 g.m^{-3} and 700 g.m^{-3} . Again, this result is consistent with the result of estimated laminar burning velocity proposed in this paper. For this reason, the value of laminar burning velocity of 60 cm.s^{-1} is considered hereafter.

The data of burning velocity obtained are then fitted by the equation proposed by Dahoe (Eq 1). The values of C and n are respectively 0.1 and 1.01. Figure 6 exposes the fit of the data with this equation. The general form of the equation is consistent with the experimental data.

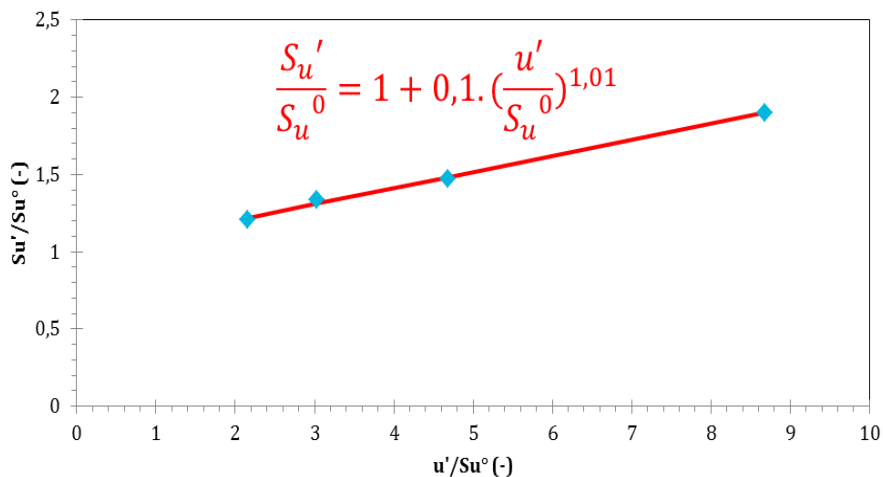


Figure 6: Relation between burning velocity and turbulence

4. Conclusions

Confined iron dust explosions have been performed using the standardized 20L explosions sphere. Iron dust with a median diameter of 5.1 μm is studied. Iron concentrations of 900 $\text{g}\cdot\text{m}^{-3}$ and 1 000 $\text{g}\cdot\text{m}^{-3}$ are tested, corresponding to fuel-rich suspensions. The ignition delay varies between the tests (40 ms, 60 ms, 80 ms and 100 ms). The initial turbulent level inside the sphere at the moment of ignition varies according to this ignition delay; the longer the ignition delay, the lower the initial turbulent level. For each configuration, two tests are realized and analyzed.

From the pressure evolution over time, two first parameters are deduced: the maximum overpressure (P_{max}) and the maximum rate of pressure rise ($(dP/dt)_{\text{max}}$). A decrease of the maximum rate of pressure rise with the rising ignition delay is observed, due to the decrease of the burning velocity with the decreasing turbulence level. A slight decrease of the maximum overpressure with the rising ignition delay is also observable, due to the increasing thermal losses at the wall corresponding to a longer combustion. For each parameter, no influence of the concentration is detected, in comparison with the repeatability of the tests. For this reason, all the tests are analyzed without considering the difference of concentrations between the tests; only the influence of the ignition delay is analyzed.

Burning velocity has been then deduced for each from the evolution of pressure inside the closed vessel. The method is based on the previous works of Faghiih and Chen (2016). Evolution of the burning velocity with the ignition delay is obtained and compared to the general equation proposed by Dahoe (2000). This form of equation fits well with the experimental data obtained. A corresponding laminar burning velocity is estimated to be 60 $\text{cm}\cdot\text{s}^{-1}$, consistent with some results of the literature.

The proposed relation between burning velocity and turbulence will be implemented in the modelling software P²REMICS. Experimental tests in a vertical tube will be realized to be compared to the results of simulations with this relation implemented. With these tests on tubes and these simulations, this proposed relation will be discussed.

Acknowledgements

The authors are grateful to IRSN (Institut de Radioprotection et de Sureté Nucléaire) for scientific and financial support to this project. The authors are grateful to Delphine Berset and Gerard Vilain (TUV SUD) for making their equipment available and for their help in carrying out the tests.

References

- Broumand M., Bidabadi M., 2013, Modeling combustion of micron-sized iron dust particles during flame propagation in a vertical duct, *Fire Safety Journal*, 59, 88–93.
- Dahoe A. E., Van der Nat K., Braithwaite M., Scarlett B., 2001, On the sensitivity of the maximum explosion pressure of a dust deflagration to turbulence, *Powder and Particle Journal*, 19, 178–196.
- Dahoe A.E., 2000, Dust explosions: a Study of Flame Propagation, PhD Thesis, Delft University of Technology, Delft, Netherlands.
- Faghiih M., Chen Z., 2016, The constant-volume propagating spherical flame method for laminar flame speed measurement, *Science Bulletin*, 61, 1296–1310.
- Kahlili I., 2012, Sensibilité, sévérité et spécificités des explosions de mélanges hybrides gaz/vapeurs/poussières. PhD Thesis, Université de Lorraine, Nancy, France.
- Santandrea A., Vignes A., Krietsch A., Perrin L., Laurent A., Dufaud O., 2019, Some key considerations when evaluating explosion severity of nanopowders, *Chemical Engineering Transactions*, 77, 235–240.
- Tang F. D., Goroshin S., Higgins A., Lee J., 2009, Flame propagation and quenching in iron dust clouds, *Proceedings of the Combustion Institute*, 32, 1905–1912.